AD-A124 456 THE EFFECTS OF CONDUCTIVITY ON HIGH-RESOLUTION IMPULSE RADAR SOUNDING ROS..(U) COLD REGIONS RESEARCH AND ENGINEERING LAB HANOVER NH R M MOREY ET AL. DEC 82 1/1

UNCLASSIFIED CRREL-82-42 NSF-DPP80-04221 F/G 8/12 NL

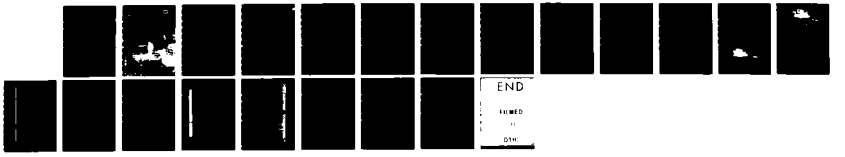

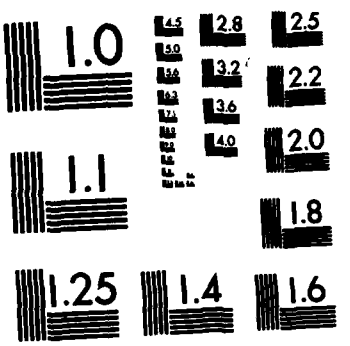

CRREL
REPORT 82-42

US Army Corps
of Engineers
Cold Regions Research &
Engineering Laboratory

The effects of conductivity on high-resolution impulse radar sounding, Ross Ice Shelf, Antarctica

For conversion of SI metric units to U.S./ British customary units of measurement consult ASTM Standard E380, Metric Practice Guide, *published by the American Society for Testing and Materials, 1916 Race St., Philadelphia, Pa. 19103.*

Cover: Mounting special liquid-filled 20-MHz antennas on Nansen Sled in preparation for radar profiling at Site J-9.

CRREL Report 82-42

December 1982

The effects of conductivity on high-resolution impulse radar sounding, Ross Ice Shelf, Antarctica

Rexford M. Morey and Austin Kovacs

Prepared for
NATIONAL SCIENCE FOUNDATION
Approved for public release; distribution unlimited

Unclassified

SECURITY CLASSIFICATION OF THIS PAGE *(When Data Entered)*

REPORT DOCUMENTATION PAGE

READ INSTRUCTIONS BEFORE COMPLETING FORM

1. REPORT NUMBER: CRREL Report 82-42	2. GOVT ACCESSION NO.: AD-A124456
3. RECIPIENT'S CATALOG NUMBER:	
4. TITLE *(and Subtitle)*: THE EFFECTS OF CONDUCTIVITY ON HIGH-RESOLUTION IMPULSE RADAR SOUNDING, ROSS ICE SHELF, ANTARCTICA	5. TYPE OF REPORT & PERIOD COVERED:
	6. PERFORMING ORG. REPORT NUMBER:
7. AUTHOR(s): Rexford M. Morey and Austin Kovacs	8. CONTRACT OR GRANT NUMBER(s): NSF DPP 80 04221
9. PERFORMING ORGANIZATION NAME AND ADDRESS: U.S. Army Cold Regions Research and Engineering Laboratory, Hanover, New Hampshire 03755	10. PROGRAM ELEMENT, PROJECT, TASK AREA & WORK UNIT NUMBERS:
11. CONTROLLING OFFICE NAME AND ADDRESS: Division of Polar Programs, National Science Foundation, Washington, D.C. 20314	12. REPORT DATE: December 1982
	13. NUMBER OF PAGES: 19
14. MONITORING AGENCY NAME & ADDRESS *(if different from Controlling Office)*:	15. SECURITY CLASS. *(of this report)*: Unclassified
	15a. DECLASSIFICATION/DOWNGRADING SCHEDULE:

16. DISTRIBUTION STATEMENT *(of this Report)*

Approved for public release; distribution unlimited.

17. DISTRIBUTION STATEMENT *(of the abstract entered in Block 20, if different from Report)*

18. SUPPLEMENTARY NOTES

19. KEY WORDS *(Continue on reverse side if necessary and identify by block number)*

Antarctica	Ice thickness
Cold regions	Polar regions
Electrical conductivity	Radar
Ice	Radar reconnaissance
Ice shelves	

20. ABSTRACT *(Continue on reverse side if necessary and identify by block number)*

A high-resolution impulse radar profiling system was evaluated for 1) detecting the existence of sea ice which coring has revealed to exist on the bottom of the Ross Ice Shelf at Site J-9, 2) detecting the preferred horizontal c-axis azimuthal direction of the sea ice crystals, using the voltage amplitude of the radar reflection from the sea ice bottom, and 3) determining the direction of the currents under an Antarctic ice shelf. A field program was conducted consisting of a surface radar survey on the Ross Ice Shelf at Site J-9 and surface and airborne radar profiling on the McMurdo Ice Shelf. The CRREL impulse radar system, operating at a center frequency of either 80 MHz or 20 MHz, was unable to detect the shelf bottom at Site J-9, which drilling revealed to be 416 m below the snow surface. The radar system was used to profile the McMurdo Ice Shelf both from the snow surface and from the air; a shelf thickness of about 275 m

DD FORM 1 JAN 73 1473 EDITION OF 1 NOV 65 IS OBSOLETE

Unclassified

SECURITY CLASSIFICATION OF THIS PAGE *(When Data Entered)*

20. Abstract (cont'd).

was easily detected. Theoretical considerations indicate that the bulk conductivity of the ice shelf at Site J-9 was higher than originally anticipated, and this limited the radar sounding depth to about 405 m when operating at a frequency of 20 MHz.

PREFACE

This report was prepared by Austin Kovacs, Research Civil Engineer, of the Applied Research Branch, Experimental Engineering Division, U.S. Army Cold Regions Research and Engineering Laboratory, and Rexford M. Morey, CRREL Expert, Nashua, N.H. Funding for the study was provided by the Division of Polar Programs, National Science Foundation, under Grant NSF 8004221.

Review comments on this report by Dr. Charles Swithinbank of the British Antarctic Survey and Dr. Samuel Colbeck of CRREL are acknowledged.

The proprietary 20-MHz liquid-filled antennas described here were designed by Rexford M. Morey for Geo-Centers Inc., who kindly loaned them to CRREL for the field program.

CONTENTS

ILLUSTRATIONS

Figure

TABLES

Table

THE EFFECTS OF CONDUCTIVITY ON HIGH-RESOLUTION IMPULSE RADAR SOUNDING, ROSS ICE SHELF, ANTARCTICA

Rexford M. Morey and Austin Kovacs

INTRODUCTION

Results of impulse radar sounding studies of sea ice have shown that where there is a preferred current direction under the ice cover the crystal structure of the ice becomes highly ordered. This includes a crystal structure with a preferred horizontal c-axis that is oriented with the local current (Kovacs and Morey 1978, 1979, 1980). The result is that when electromagnetic energy is radiated, in the megahertz frequency band, from a dipole antenna in which the electric field (E-field) is oriented perpendicular to the azimuth of the c-axis of the ice crystals, a weak bottom reflection (or none at all) is detected. But when the E-field is oriented parallel with the c-axis there is a strong reflection from the ice bottom. It has also been found that the frequency dispersion of anisotropic sea ice varies in the horizontal plane. This was demonstrated by the center frequency of the reflected signal spectrum from the ice bottom, which was maximum when the E-field was parallel to the preferred c-axis direction and minimum when the E-field was perpendicular to it.

Coring through the Ross Ice Shelf at Site J-9 (Fig. 1), Zotikov (1979) found the shelf to be 416 m thick, and from examining the ice core recovered noted a bottom layer composed of 6 m of saline (sea) ice. He also discovered that the sea ice structure consisted of long ice crystals with a preferred horizontal c-axis. This discovery suggests that it should be possible, using the CRREL impulse radar system, to detect the existence of the sea ice layer at Site J-9. And, through analysis of the amplitude of the reflected wavelet from the sea ice/water interface versus antenna E-field azimuth orientation, it should be possible to determine the alignment of the current at the ice/water interface.

We have used the CRREL impulse radar successfully in the Arctic to profile sea ice thickness and to investigate sea ice anisotropy arising from the preferred horizontal azimuth alignment of the c-axes of the ice crystals at the bottom of the ice cover (Kovacs and Morey 1978, 1979, 1980). In addition, we have used the system in the Antarctic to investigate the slope and lateral extent of the brine infiltration layer in the McMurdo Ice Shelf, the thickness of the shelf, and saline ice growth under the floating Koettlitz

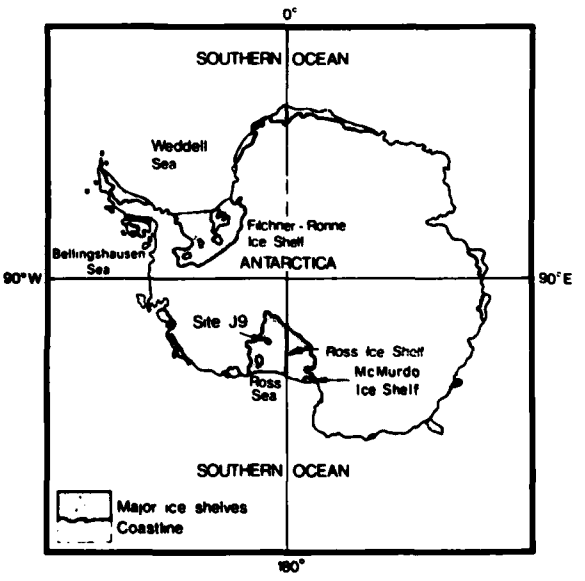

Figure 1. Map of the Ross Ice Shelf showing Site J-9 and the McMurdo Ice Shelf survey locations.

Glacier ice tongue (Kovacs and Gow 1975, 1977, Gow and Kovacs 1979, Kovacs et al. 1982). Based upon these results and preliminary radar range calculations, we concluded that the radar system could also detect the sea ice growth layer under the Ross Ice Shelf at Site J-9 and the preferred c-axis azimuth of the ice crystals. Since the alignment of the crystal c-axis in sea ice has been found to be parallel with the current at the ice boundary we also expected to be able to predict the alignment of the current at the ice/water interface. If the radar sounding at Site J-9 was successful, the radar data were to be correlated with seawater current information to be measured at the bottom of the drill hole at Site J-9 by Norwegian investigators. The optimum goal was to demonstrate the ability to profile the thickness of the sea ice growth layer over a larger area of the Ross Ice Shelf to determine where sea ice is growing or ablating and where the glacial ice may be melting. This information is important in understanding the mass balance of the ice shelf.

PROFILING SYSTEM

The impulse radar system used has been described in the literature previously referenced. In short, it consists of timing electronics which clock an impulse generator and sampling head. The impulse source generates 60- to 150-V impulses with a band width of nearly 200 MHz at a selectable repetition rate of 12.5, 25, or 50 kHz and a pulse width of 3 to 10 ns (depending upon the antenna and therefore the frequency used). The impulse is fed to a transmitting-receiving antenna which radiates an electromagnetic (EM) wavelet into the underlying material.

Three different antennas, with center frequencies of 20, 80 and 300 MHz, were used. The highest-frequency antenna was for high resolution profiling. The lower frequency antennas were used for signal amplitude reflection measurements from the sea ice bottom versus antenna E-field orientation. The reflected radar EM wavelet, for example from the ice shelf bottom, is displayed on an oscilloscope and graphic recorder. The signal data are also stored on an analog tape recorder for later playback and data processing. The EM signal information recorded is the travel time to and from the various reflecting surfaces and the voltage amplitude of the reflected EM wavelet.

In the laboratory the recorded data can be played back and analyzed on a frequency spectrum analyzer. In this process the exact time of flight to, for example, the glacial ice/sea ice or the sea ice/water boundary can be obtained, as well as the voltage amplitude and frequency content of the signal from the various interfaces. The time-of-flight information is used in calculating ice shelf thickness. The reflected amplitude data can be used to determine the azimuth at which the maximum reflection occurred at the sea ice/water interface, and thus to find the under-ice current alignment (Kovacs and Morey 1978, 1979, 1980).

THEORETICAL CONSIDERATIONS

The electromagnetic properties of all materials are described by the following constitutive parameters: effective conductivity σ_e, effective permittivity $\epsilon_e = \epsilon_r \cdot \epsilon_0$, and effective permeability $\mu_e = \mu_r \cdot \mu_0$, where ϵ_r and μ_r are the relative dielectric constant and relative permeability, $\epsilon_0 = 8.85 \times 10^{-12}$ farads/meter (F/m), and $\mu_0 = 4\pi \times 10^{-7}$ henrys/meter (H/m). Plane wave propagation is governed by the complex propagation constant γ, which may be determined from

$$\gamma = \alpha + j\beta = [-\omega^2 \mu \epsilon_e + j\omega\mu\sigma_e]^{1/2} \qquad (1)$$

where

β = real phase constant
α = attenuation constant
$\omega = 2\pi f$ = angular frequency
f = frequency

As the radar pulse progresses through the ice with a phase velocity $v_m = \omega/\beta$, it suffers an exponential attenuation with an attenuation constant α. Thus, the attenuation A in decibels/meter (dB/m) is

$$A = 20\,\alpha \log_{10}(e)\,. \qquad (2)$$

The pulse is partially reflected at an interface between two different materials (e.g. ice and seawater), the reflection coefficient ρ being

$$\rho = \frac{\eta_2 - \eta_1}{\eta_2 + \eta_1} \qquad (3)$$

where the complex characteristic impedances η of the media are given by

$$\eta = \frac{j\omega\mu}{\gamma}\,. \qquad (4)$$

Studies of the electromagnetic probing of snow and ice require a firm understanding of the complex dielectric constant of the materials as a function of frequency, temperature, and impurity content. The relative complex dielectric constant for ice is adequately expressed by the following Debye equation:

$$\epsilon_r^* = \epsilon_r' - j\epsilon_r'' = \epsilon_{r\infty} + \frac{\epsilon_{rs} - \epsilon_{r\infty}}{1 + j\omega\tau} - j\,\frac{\sigma_{DC}}{\omega\epsilon_0} \quad (5)$$

where

$\epsilon_{r\infty}$ = relative high frequency dielectric constant = 3.15 ± 0.05
ϵ_{rs} = relative static dielectric constant (temperature-dependent)
τ = relaxation time (temperature-dependent)
σ_{DC} = zero frequency conductivity

The form of eq 5 is presented to explicitly evaluate the effect of DC conductivity on the properties of polar ice, since for pure, solid ice there is no DC conductivity. The real effective parameters in eq 1, σ_e and ϵ_e, are related to the complex constitutive parameters by:

$$\sigma_e = \sigma' + \omega\epsilon'' \text{ (S/m)} \quad (6)$$

$$\epsilon_e = \epsilon' - \frac{\sigma''}{\omega} \doteq \epsilon' \text{ (F/m)} \quad (7)$$

where ϵ' equals the real part of the dielectric constant, and the imaginary part of the conductivity σ'' equals zero at the frequencies of interest. The effective conductivity is a function of both σ', which is the zero frequency conductivity, and ϵ'', which is the dielectric relaxation loss factor due to the oscillation of dipolar molecules in a time-varying electric field. Thus we specifically separate the two energy dissipation processes in ice, namely conduction and relaxation. The DC conductivity of ice is a measure of the impurities within the ice.

The relaxation time, τ, is temperature-dependent and is also dependent upon the concentration of impurities in the ice (Gross et al. 1978). For "pure" ice τ is well approximated by (King and Smith 1981)

$$\tau = \tau_0 \exp(E/RT) \quad (8)$$

where

$\tau_0 = 5.3 \times 10^{-16}$ s
E = activation energy ≈ 13.25 kcal/mole
R = gas constant = 1.9865 cal/K-mole

Table 1 lists some representative materials and their electromagnetic parameters at a frequency of 80 MHz. The conductivity has the greatest influence on the attenuation, while the velocity of propagation in the material v_m is mostly a function of the relative dielectric constant.

The maximum range of an ice-probing radar system is a function of the system parameters, the target or interface parameters, and the electromagnetic properties of the material being probed. The radar equation or the system performance factor Q is

$$Q = 10 \log \left[\frac{E_T \cdot E_R \cdot G_T \cdot G_R \cdot v_m^2 \cdot g \cdot \sigma \cdot e^{-4\alpha L}}{64\,\pi^3 f^2 L^4} \right] \quad (9)$$

where

E_T and E_R = transmitting (T) and receiving (R) antenna efficiency
G_T and G_R = transmitting (T) and receiving (R) antenna gain
v_m = velocity of propagation in the medium
g = backscatter gain of target
σ = target scattering cross-sectional area
α = attenuation coefficient of medium (eq 1)
L = range to target
f = frequency of signal

or

$$Q = 10 \log \left[\frac{P_{min}}{P_{in}} \right] \quad (10)$$

where

P_{min} = minimum detectable signal power
P_{in} = power input to the transmitting antenna

The effective conductivity of polar ice is variable and depends on temperature and impurity content. Published values for the bulk DC conductivity of polar ice range between 7×10^{-6} S/m and 5×10^{-5} S/m (Bentley 1977, Robin et al. 1969). Therefore, the attenuation in polar ice may be between 6.44×10^{-3} and 4.60×10^{-2} dB/m at 80 MHz.

Using data from Table 1 and eq 3 and 4 the reflection coefficient at a boundary between several different materials was determined (Table 2). In Table 2 the magnitude of the reflected signal is seen to be greater at a glacial ice/seawater boundary than at a glacial ice/sea ice boundary. A glacial ice/seawater boundary would therefore be detectable at a greater distance than a glacial ice/sea ice boundary.

Resistivity measurements made by Bentley (1977) at Site J-9 indicated that the bulk DC conductivity was 1.4×10^{-5} S/m. Prior to our field trip this information was used to estimate the maximum depth of penetration (using eq 9 and 10 to estimate maximum L) for the radar antenna systems we used (to be discussed later). The calculated maximum depth of penetration was greater than 600 m with and without sea ice on the bottom at sounding frequencies of 20 and 80 MHz. Thus we expected to see the bottom of the ice shelf at Site J-9.

Table 1. Approximate electromagnetic parameters at 80 MHz.

Material	σ_e *(S/m)*	μ_r	ϵ_r	A *(dB/m)*	v_m *(m/ns)*	n *(ohms)*
Air	0	1	1	0	0.30	377
Polar ice	10^{-5}	1	3.15	9.2×10^{-3}	0.168	$211.7 + j\,0.075$
Sea ice	10^{-1}	1	6	42.8	0.078	$62 + j\,48$
Seawater*	4	1	81	295	0.014	$9.2 + j\,8.5$
Fresh water*	10^{-3}	1	81	0.18	0.033	$41.9 + j\,0.058$

* At 20°C.

Table 2. Reflection at a smooth boundary.

Reflector boundary	*Refl. coeff. (ρ)*	*Refl. magnitude*	*Phase angle (β)*
Air-ice	$-0.28 + j\,0.0002$	28%	180°
Shelf ice-seawater	$-0.91 + j\,0.073$	92%	175°
Shelf ice-sea ice	$-0.50 + j\,0.26$	56%	152°

FIELD PROGRAM

In preparation for the Site J-9 field program several changes and modifications were made to the CRREL impulse radar system in order to improve its performance and thus increase the maximum radar range. The antennas, each operating at a different center frequency (20, 80 and 300 MHz), were tested. A preamplifier was placed at the front ends of the receivers, providing an additional 10 to 15 dB of gain. Generally, this radar system, like most other radar subsurface sounding systems, uses one antenna for transmitting and receiving simultaneously. In our study two sets of matched dipole antennas operating at either 80 or 300 MHz were used, both transmitting and receiving simultaneously (Fig. 2). Theoretically this would provide a 6-dB gain in system performance. Experimental results indicated about a 4.5-dB improvement.

The 20-MHz system consisted of special liquid-filled antennas, one for transmitting and one for receiving (Fig. 3). Each antenna consisted of a plastic tube 10 cm in diameter and about 3 m long. A uniquely configured copper dipole element was

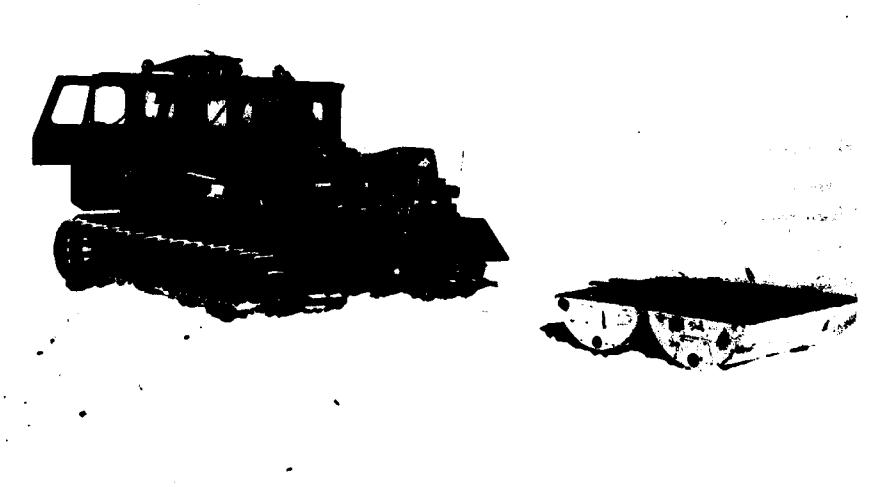

Figure 2. Two 80-MHz antennas being towed by tracked vehicle which contains electronic recording equipment.

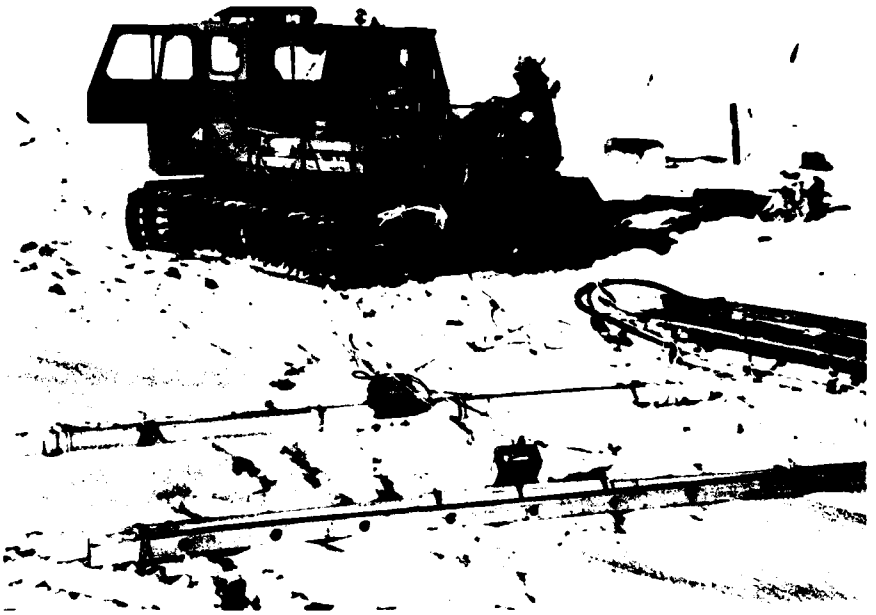

Figure 3. Twenty-MHz transmitting and receiving antennas at Site J-9.

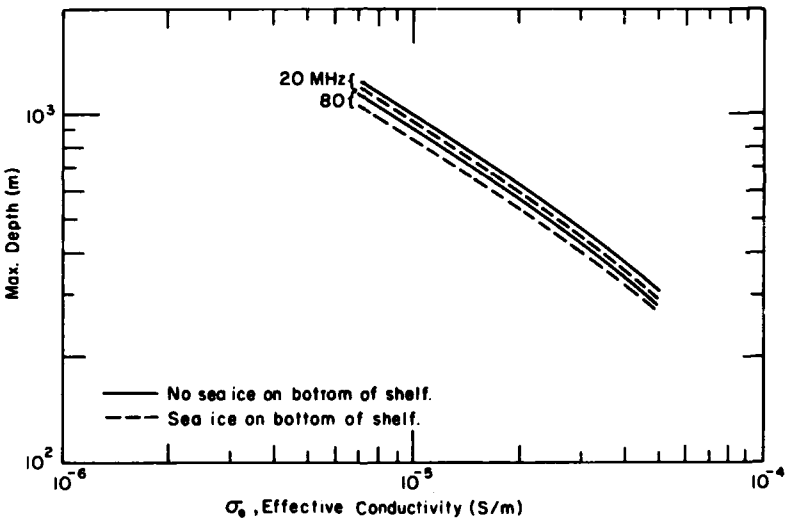

Figure 4. Maximum ice/water interface depth detectable as a function of the effective (bulk) conductivity of an ice shelf having a smooth bottom.

Table 3. Radar parameters for calculating maximum range.

Radar parameter	*Center frequency*		
	20 MHz	*80 MHz*	*300 MHz*
P_{in} (peak watts)	2.5×10^3	50	12
P_{min} (watts)	2.5×10^{-8}	5×10^{-11}	1.2×10^{-11}
Q	-110 dB	-120 dB	-120 dB
$E_T = E_R$	-13 dB	-13 dB	-13 dB
$G_T = G_R$	2 dB	2 dB	2 dB

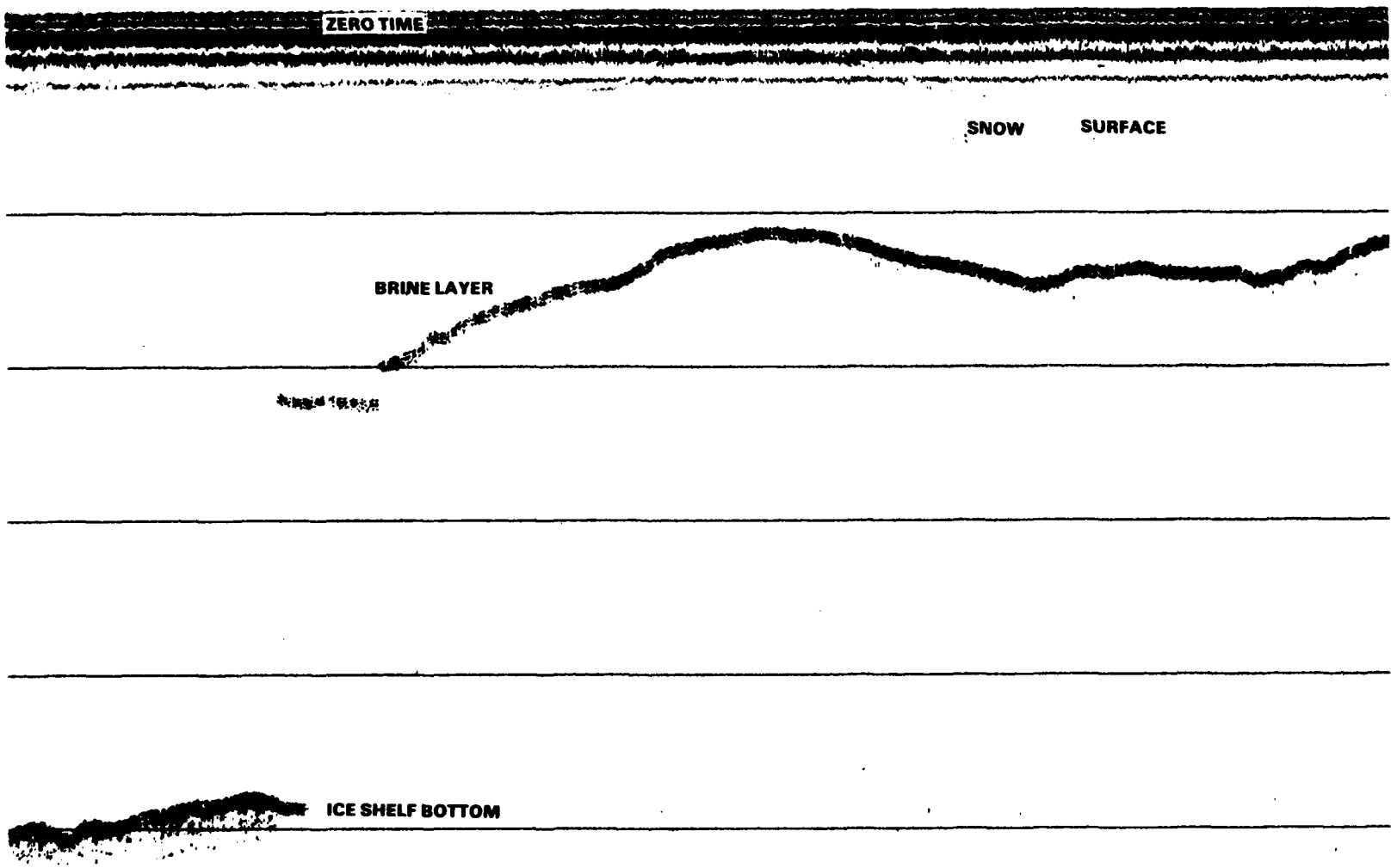

Figure 5. Portion of graphic record of radar sounding profile obtained during airborne survey of the McMurdo Ice Shelf. Time between scan lines is about 270 ns. The brine layer is the top of the zone of seawater infiltration in the McMurdo Ice Shelf as discussed in Kovacs et al. (1982). The time-varying undulation in the radar record is due to vertical changes in helicopter flight altitude.

supported along the center axis of the plastic tube, which was divided into several chambers. A low-loss liquid filled one chamber and a high-loss liquid the other. The purpose of the dielectric liquid was to make the antenna electrically longer than its physical length and thus radiate lower frequencies. The high-loss dielectric liquid tended to damp out pulse ringing on the antenna.

Table 3 lists the radar parameters used for calculating the maximum radar range. The 80- and 300-MHz system values in Table 3 are based upon the dual transceiver antenna configuration. The maximum radar range as a function of conductivity for the 20- and 80-MHz antennas is plotted in Figure 4. Two models are considered, one without any sea ice on the ice shelf bottom and one with 6 meters of sea ice. The maximum radar range is shown to be very sensitive to the effective conductivity of the shelf ice.

Before leaving for Site J-9 we tested the radar system on the McMurdo Ice Shelf. We were able to penetrate about 250 m of the shelf and receive fairly strong ice/water reflections at all three radar sounding frequencies. However, the weakest bottom return occurred at 300 MHz. Measurements were also made on the McMurdo Ice Shelf using a single 80-MHz antenna suspended from a helicopter flown at an altitude of 10–15 m. Shelf thicknesses of up to 275 m were continuously profiled (Fig. 5). This was the maximum shelf thickness encountered on the flight.

The ice shelf thickness at Site J-9 is 416 m (Zotikov 1979). Radar profile traverses extending up to 2 km from Site J-9 were made with both the 20-MHz and the dual 80-MHz antennas. Neither antenna system appeared to detect the glacial ice/sea ice boundary or the sea ice/seawater boundary.

DISCUSSION

Since our earlier estimates indicated that we should have "seen" the bottom of the ice shelf at Site J-9, we reevaluated the radar range equation (eq 9) and the parameters that contributed to it, and also used more recent information (Jezek 1980) on the attenuation characteristics of the ice shelf at Site J-9.

Using the temperature-depth profile at Site J-9, Jezek (1980) determined the two-way absorption loss to be 15 dB ± 1 at 35 MHz. Equation 5 was used to calculate ϵ_r'' as a function of temperature for "pure" ice ($\sigma_{DC} = 2.1 \times 10^{-8}$ S/m) at 35 MHz, where the values for ϵ_{rs} and τ were taken from King and Smith (1981). The effective (bulk) conductivity σ_e was then calculated using eq 6 for "pure" ice and for the ice shelf at Site J-9 with a bulk DC conductivity of 1.4×10^{-5} S/m as found by Bentley (1977). Table 4 lists the ϵ_{rs} and τ vs temperature values used in the analysis along with the calculated σ_e results. Figure 6 is a plot of σ_e at 35 MHz as a function of temperature. For the 416-m-thick ice shelf at Site J-9, a two-way attenuation of 15 dB as determined by Jezek (1980) represents an effective (bulk) conductivity of 1.9×10^{-5} S/m (assuming no impurities in the ice shelf). And, for a DC conductivity of 1.4×10^{-5} S/m as found by Bentley (1977) at Site J-9, the effective (bulk) conductivity of the ice shelf is estimated to be 3.3×10^{-5} S/m at 35 MHz (Fig. 6). Note that both conductivity and relaxation time are concentration-dependent (Gross et al. 1978). Therefore, the difference in the two σ_e values (1.9×10^{-5} vs 3.3×10^{-5} S/m) given above may be due to impurity effects. Since we do not know the type of impurities or their concentrations at Site J-9, we cannot include this effect on the relaxation time. However, impurities within the ice tend to decrease τ (increasing ϵ_r''), and thus would increase σ_e beyond the value derived from Jezek's data.

Figure 7 is a plot of effective conductivity as a function of frequency for two different temperatures. Above 100 kHz the effective conductivity is frequency-independent but is dependent on temperature and impurity content. If one assumes that the average temperature of an ice sheet such as the Ross Ice

Table 4. Static dielectric constant, relaxation time, and imaginary part of relative dielectric constant of pure ice ($\sigma_{DC} = 2.1 \times 10^{-8}$ S/m) at 35 MHz.

T (°C)	ϵ_{rs}	τ (s)	ϵ_r''	σ_e (S/m) ($\sigma_{DC} = 2.1 \times 10^{-8}$)	σ_e (S/m) ($\sigma_{DC} = 1.4 \times 10^{-5}$)
0	91.1	2.05×10^{-5}	1.95×10^{-2}	3.8×10^{-5}	5.20×10^{-5}
-5	93.4	3.25×10^{-5}	1.26×10^{-2}	2.46×10^{-5}	3.85×10^{-5}
-10	95.0	5.13×10^{-5}	8.15×10^{-3}	1.59×10^{-5}	2.99×10^{-5}
-15	96.1	8.70×10^{-5}	4.87×10^{-3}	9.5×10^{-6}	2.35×10^{-5}
-20	97.2	1.49×10^{-4}	2.89×10^{-3}	5.6×10^{-6}	1.96×10^{-5}
-25	98.2	2.55×10^{-4}	1.71×10^{-3}	3.35×10^{-6}	1.73×10^{-5}

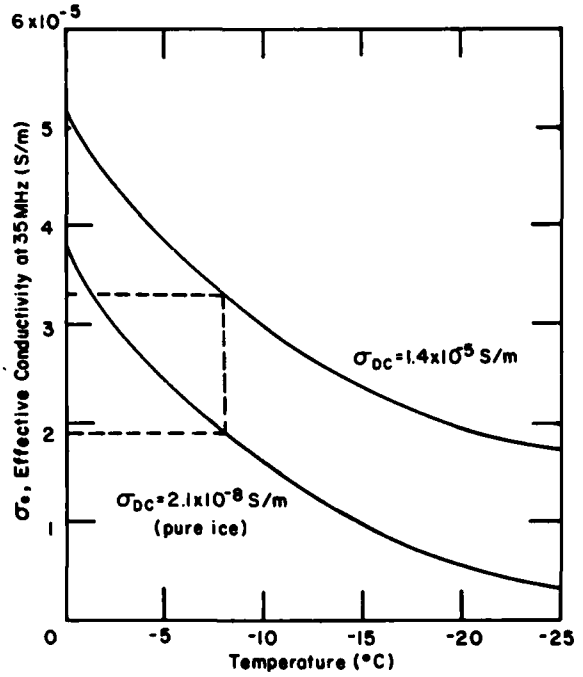

Figure 6. Plot of effective (bulk) conductivity at 35 MHz as a function of temperature.

Shelf is constant over large areas, then the effective conductivity is essentially a function of impurity content.

From the absorption loss information of Jezek (1980), we have now made an estimate of the apparent high frequency (>100 kHz) effective (bulk) conductivity of 3.3×10^{-5} S/m for the ice shelf at Site J-9. This value was determined by correcting the bulk DC conductivity of Bentley (1977) for temperature and frequency effects as depicted in Figure 7. Using $\sigma_e = 3.3 \times 10^{-5}$ S/m we can now recalculate the maximum sounding depth of our 20-MHz radar system at Site J-9 to be about 425 m with no sea ice layer on the ice shelf bottom and about 405 m with 6 m of sea ice on the bottom (Fig. 4). The above analysis indicates that our radar equipment was just at the limit of being able to detect the shelf bottom at Site J-9. The maximum calculated depth of penetration for the 300-MHz system is about 260 m for an ice shelf having a $\sigma_e = 3.3 \times 10^{-5}$ S/m and a smooth ice bottom with no sea ice. Thus the weak reflection obtained from the ice/water interface on the McMurdo Ice Shelf at a depth of about 250 m, as previously discussed, was apparently due to the fact that this system was approaching its maximum sounding depth.

At Site J-9 we did observe many internal layers and parabolic reflections believed to be signatures of buried crevasses (Fig. 8). The crevasses are believed to have developed upstream of Site J-9 and to have become buried by subsequent snow accumulations during the years they were moving toward the site. The tops of these relic crevasses are calculated to be about 46 m below the snow surface. Figure 9 shows concave undulations in the internal layers above and between relic crevasses. Clough (1975) and Jezek (1980) reported on bottom crevasses in the Ross Ice Shelf and at Site J-9 using radio-echo sounding techniques. Because of the length of the pulse used in their radar systems, near-surface details were lost. Surface topography at Site J-9 does not indicate the presence of near-surface relic crevasses or bottom crevasses. However, Jezek (1980) suggested that as some bottom crevasses form, a surface depression develops between them. He speculated that the shelf surface between the water-filled bottom crevasses would settle by about 13 m, forming a concave depression. Our radar profiles at Site J-9 support this concept, and we propose that surface crevasses may have formed as a result of bottom crevassing, as depicted in Figure 10.

As pointed out earlier, the maximum detectable bottom depth for a radar sounding system is in part

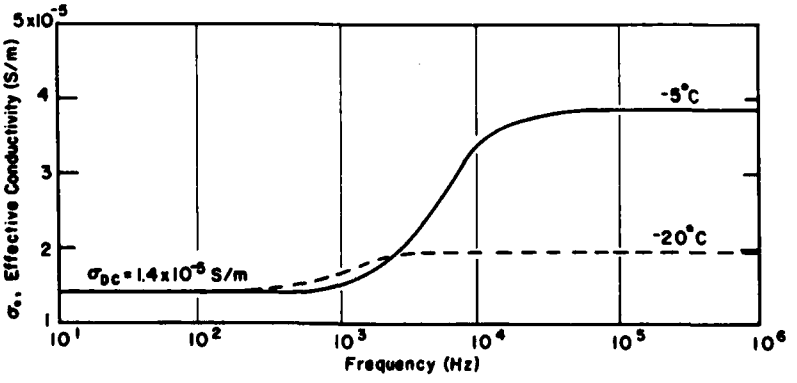

Figure 7. Plot of effective (bulk) conductivity as a function of frequency for two different temperatures.

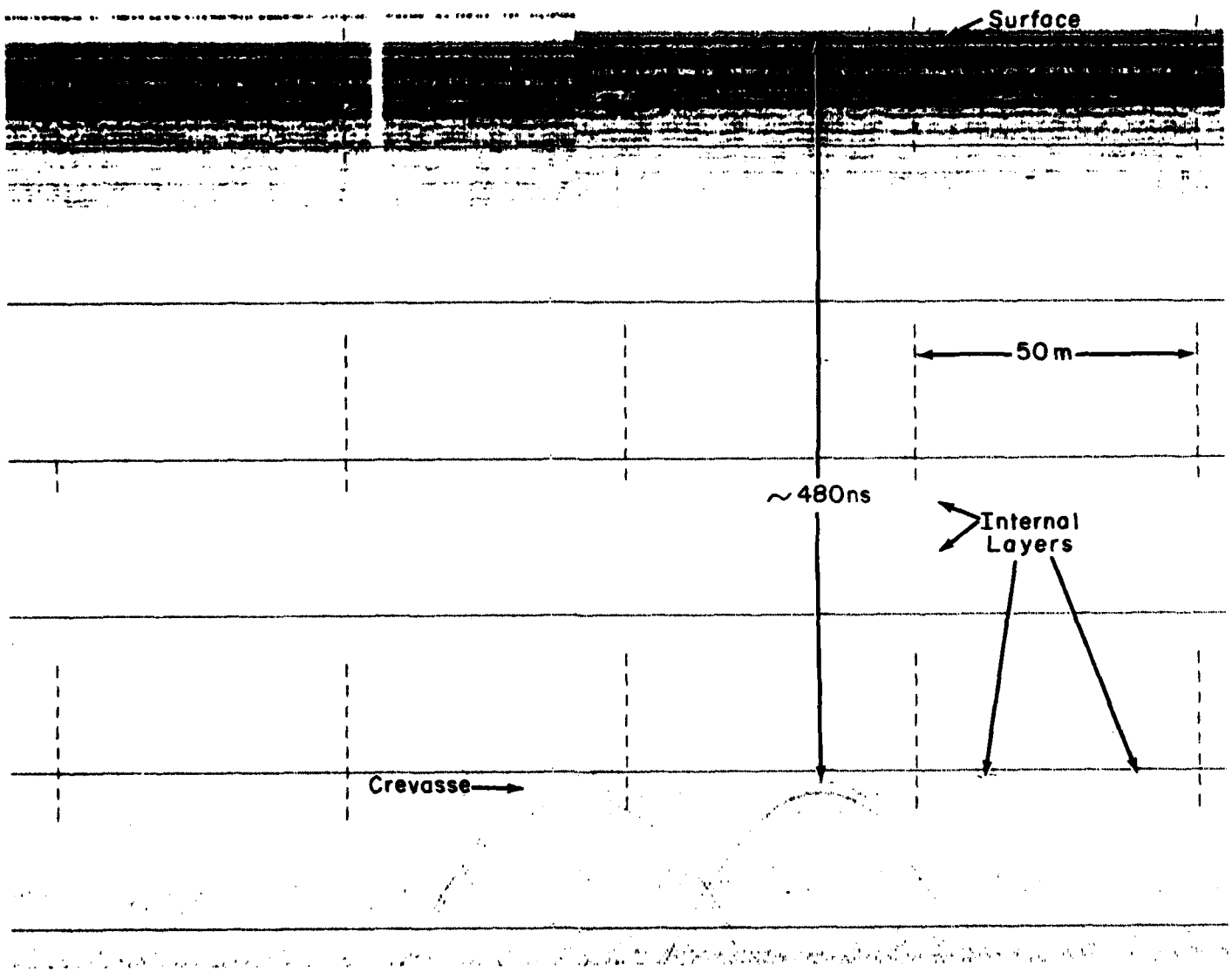

Figure 8. Graphic record of radar profile over two of the many "side by side" buried crevasses observed near Site J-9. Time between horizontal scale lines is 100 ns.

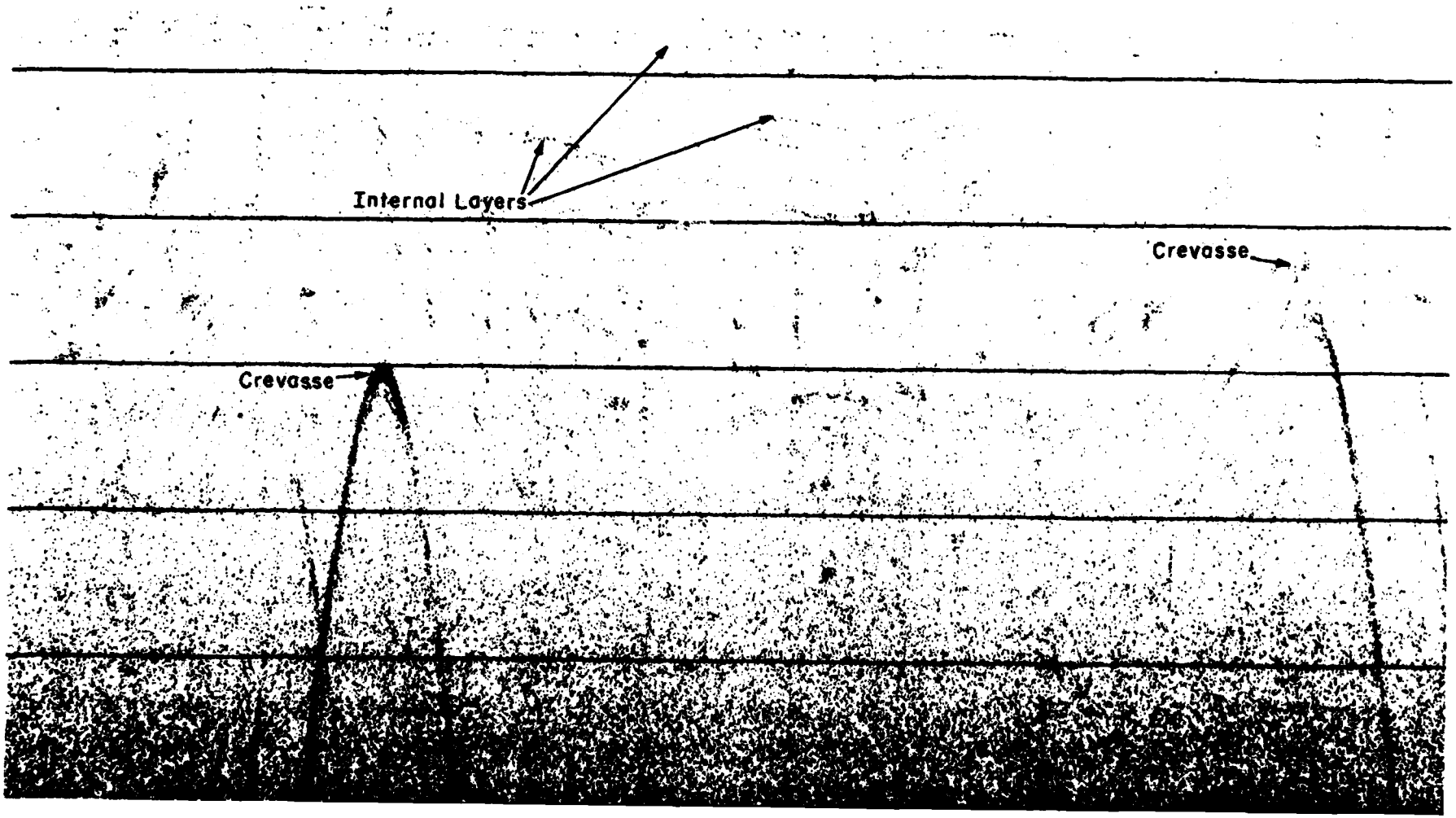

Figure 9. Graphic record of radar sounding profile showing concave undulations in the internal layers above and between relic crevasses near Site J-9. Surface return not shown. Time between horizontal scale lines is 100 ns.

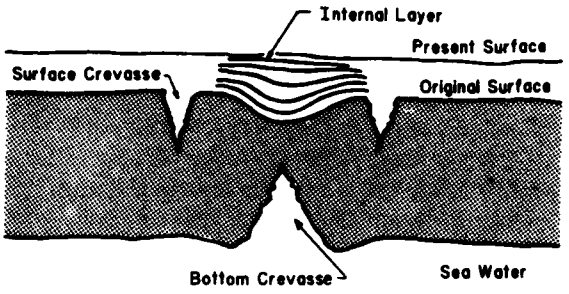

Figure 10. Schematic of proposed method in which some surface crevasses are formed as a result of bottom crevassing.

a function of the effective conductivity of the ice (Fig. 4). The conductivity of the ice is a function of its temperature and impurity content. Many radar sounding profiles obtained from aircraft flights over the Ross Ice Shelf have sections of data showing an absence of bottom echo (Jezek 1980). Neal (1982) evaluated small-scale roughness on the bottom of the Ross Ice Shelf and its effect on radio echo fading patterns. The lack of ice shelf bottom return is also attributed to such things as brine infiltration, crystal fabric alignment, and debris within the ice. We suggest that bottom echo fading and extinction in radio echo-sounding may also be due to changes in the bulk DC conductivity of the ice shelf. Bentley (1977) pointed out that measurements near Roosevelt Island and at Byrd Station indicate a DC conductivity one-half that at Site J-9, or about 7×10^{-6} S/m. This represents an effective (bulk) conductivity of about 1.6×10^{-5} S/m at our radar sounding frequencies. Referring to Figure 4, at the latter conductivity the maximum depth of penetration of our radar system operating at 20 MHz would be about 720 m instead of about 425 m at Site J-9 where the apparent effective (bulk) conductivity is 3.3×10^{-5} S/m. Different radar systems will, of course, have different performance characteristics and, therefore, the curves in Figure 4 will be shifted vertically up or down depending on the system used. However, relatively small changes in bulk conductivity will change the amplitude of shelf bottom echos.

The question then arises as to what mechanism causes variations in conductivity in the ice at different locations. One explanation is that some difference in the densification or strain history of the ice may cause variations in conductivity, since it is assumed that the snow that fell over large areas contained about the same impurities. However, there is evidence that accumulation rates and microparticle distribution vary considerably over regions of the Antarctic (Thompson and Mosley-Thompson 1982). Jezek (1980) pointed out that the amplitude of bottom reflections seen in airborne radar sounding data taken on the Ross Ice Shelf changes from strong to very poor. For example, strong bottom returns are seen for the ice emerging from East Antarctic outlet glaciers feeding the Ross Ice Shelf, whereas weak radar reflections are seen for the ice shelf bottom in areas between these outlet glaciers. In addition, the radar bottom reflections diminish in intensity as the ice moves downstream toward the Ross Sea. A possible implication is that the conductivity of the ice is less in the outlet glaciers and that local storms deposit more sea salts near the edge of the Ross Ice Shelf, increasing the shelf conductivity locally. Jezek also mentions the existence of a few strong multiple bottom reflections near Roosevelt Island—stronger than those near Site J-9. The reported bulk DC conductivity at Site J-9 was about twice that near Roosevelt Island. Thus, the difference in radio-echo strength may be due to local and regional changes in the bulk DC conductivity of the ice due to variations in impurity content.

LITERATURE CITED

Bentley, C.R. (1977) Electrical resistivity measurements on the Ross Ice Shelf. *Journal of Glaciology,* 18(78): 15-35.

Clough, J.W. (1975) Bottom crevasses in the Ross Ice Shelf. *Journal of Glaciology,* 15(73): 457-485.

Gow, A.J. and A. Kovacs (1979) Subsurface measurements of the McMurdo Ice Shelf. *Antarctic Journal of the United States,* 14(5): 79-80.

Gross, G.W., I.C. Hayslip and R.N. Hoy (1978) Electrical conductivity in relaxation in ice crystals with known impurity content. *Journal of Glaciology,* 21(85): 143-160.

Jezek, K.C. (1980) Radar investigations of the Ross Ice Shelf, Antarctica. Ph.D. thesis, University of Wisconsin–Madison (unpublished), 204 pp.

King, R.W.P. and G.S. Smith (1981) *Antennas in Matter.* Cambridge, Massachusetts: MIT Press.

Kovacs, A. and A.J. Gow (1975) Brine infiltration in the McMurdo Ice Shelf, McMurdo Sound, Antarctica. *Journal of Geophysical Research,* 80(15): 1957-1961.

Kovacs, A. and A.J. Gow (1977) Subsurface measurements of the Ross Ice Shelf, McMurdo Sound, Antarctica. *Antarctic Journal of the United States,* 12(4): 146-148.

Kovacs, A. and R.M. Morey (1978) Radar anisotropy of sea ice due to preferred azimuthal orientation of the horizontal c-axes of ice crystals. *Journal of Geophysical Research,* 83(C12): 6037-6046.

Kovacs, A. and R.M. Morey (1979) Anisotropic properties of sea ice in the 50-150 MHz range. *Journal of Geophysical Research*, 84(C9): 5749-5759.

Kovacs, A. and R.M. Morey (1980) Investigation of sea ice anisotropy, electromagnetic properties, strength, and under-ice current orientation. U.S. Army Cold Regions Research and Engineering Laboratory, CRREL Report 80-20, 18 pp.

Kovacs, A., A.J. Gow and J. Cragin (1982) The brine zone in the McMurdo Ice Shelf, Antarctica. Third International Symposium on Antarctic Glaciology, The Ohio State University, Columbus, Ohio. *Annals of Glaciology*, 3: 166-171.

Neal, C.S. (1982) Radio echo determination of basal roughness characteristics on the Ross Ice Shelf. *Annals of Glaciology*, 3: 216-221.

Robin, G. de Q., S. Evans and J.T. Bailey (1969) Interpretation of radio echo sounding in polar ice sheets. *Philosophical Transactions of the Royal Society, London*, Ser. A, 265(1166): 437-505.

Thompson, L.G. and E. Mosley-Thompson (1982) Spatial distribution of microparticles within Antarctic snowfall. *Annals of Glaciology*, 3: 300-306.

Zotikov, I.A. (1979) Antifreeze-thermal drilling for core through the central part of the Ross Ice Shelf (J9 camp), Antarctica. U.S. Army Cold Regions Research and Engineering Laboratory, CRREL Report 79-24, 12 pp.

A facsimile catalog card in Library of Congress MARC format is reproduced below.

Morey, Rexford M.
The effects of conductivity on high-resolution impulse radar sounding, Ross Ice Shelf, Antarctica / by Rexford M. Morey and Austin Kovacs. Hanover, N.H.: Cold Regions Research and Engineering Laboratory; Springfield, Va.: available from National Technical Information Service, 1982.
iv, 19 p., illus.; 28 cm. (CRREL Report 82-42.)
Prepared for National Science Foundation by U.S. Army Cold Regions Research and Engineering Laboratory.
Bibliography: p. 11.
1. Antarctica. 2. Cold regions. 3. Electrical conductivity. 4. Ice. 5. Ice shelves. 6. Ice thickness. 7. Polar regions. 8. Radar. 9. Radar reconnaissance. I. Kovacs, A. II. United States. Army. Corps of Engineers. III. Cold Regions Research and Engineering Laboratory, Hanover, N.H. IV. Series: CRREL Report 82-42.

☆U.S. GOVERNMENT PRINTING OFFICE: 1982 – A-2294/326